



Spectral beam combining of diode lasers extended into the non-SBC direction

JUN ZHANG,^{1,2,*} HANGYU PENG,^{1,2,3} JIYE ZHANG,¹ JINGBO WANG,¹ JINLIANG HAN,^{1,2} YUXIN LEI,¹ LI QIN,¹ AND LIJUN WANG¹

¹State Key laboratory of Luminescence and Application, Changchun Institute of Optics, Fine Mechanics and Physics, Chinese Academy of Sciences, Changchun 130033, China

²University of Chinese Academy of Sciences, Beijing 100049, China

³penghy@ciomp.ac.cn

*jzh_ciomp@163.com

Abstract: An extended spectral beam combining (SBC) configuration that folds the optical path of the combining laser into the non-SBC direction and doubly narrows the SBC spectrum by introducing a right angular prism is proposed. Similar combined power and beam quality but half of the spectral width and a smaller size are demonstrated by comparing the standard SBC with the proposed SBC of the same 800nm laser bar. It provides an effective way to miniaturize the SBC size, improve the SBC stability and compress the SBC spectrum simultaneously. As far as we know, this study is also the first to report on folding the SBC optical path to the non-SBC direction, which provides a new idea for the SBC source.

© 2022 Optica Publishing Group under the terms of the [Optica Open Access Publishing Agreement](#)

1. Introduction

SBC is a promising way to improve beam quality and scale brightness of high-power diode lasers [1,2]. The SBC lasers are capable of achieving high power (equals to the sum of all the emitter power) and good beam quality (the same as that of a single emitter) with the help of the external feedback and the grating dispersion [3,4]. This way greatly promotes the brightness from 100 MW/cm²/sr to 10 GW/cm²/sr [5]. F. Villarreal et al. applied the SBC technology to diode bars to demonstrate the SBC power of 435 W with the beam parameter product (BPP) of 1.8 mm × mrad in the 400 nm region, and they also proposed an approach for a 6 kW / 50 μm fiber coupled laser in the 875 - 1000 nm spectral region [6]. H. Yu et al. reported an SBC fiber coupled laser diode module for pumping Yb-doped fiber lasers by employing gratings with the line density of 1851 lines/mm, and this module can deliver more than 350 W at 976 nm in a 50 μm / NA 0.15 fiber [7]. M. Haas et al. reported a 1.1 kW SBC laser diode module with a symmetrical BPP of about 6 mm × mrad based on a thin film filter as the dispersive element and a -1st order transmission grating (TG) as the laser combiner [8]. Z. D. Zhu et al. developed a 976 nm SBC diode laser with a narrow linewidth of 0.48 nm by using a transform lens (TL) with a long focal length of 1.5 m and an 1851 lines/mm TG [8]. B. H. Wang et al. reported SBC of 25 single emitters by using a 1600 lines/mm TG, and this configuration has an average power of about 220 W, a linewidth of less than 9 nm, and a beam quality similar to that of a single emitter [9]. The beam diffracted by the grating is in the same plane as the optical path in front of the grating, regardless whether it is an SBC structure based on a TG or a reflection grating, which leads to a very large structural size in the SBC direction. The output coupler (OC), as the front cavity mirror of the external resonator, plays a key role in the stability of the SBC performance. However, the OC in the structure previously reported was always located at the edge of the SBC structure. Moreover, the OC is usually far away from the grating with a distance of up to several hundred millimeters to reduce crosstalk effects [10]. Thus, the OC is easily affected by environment, stress, and other factors, which eventually deteriorates the SBC performance. In addition, the combining laser

only undergoes a single diffraction on the grating in the SBC structure, which limits the ability to compress the spectral linewidth.

A novel SBC structure is proposed, which extends the combined laser into the non-SBC direction and realizes a second diffraction by introducing a right angular prism (RP). The second diffracted laser coincides with the central optical axis at the first incident on the grating in the SBC direction, but a displacement occurs in the non-SBC direction. The grating can be directly installed behind the transformation lens, and all the laser beams overlap on the grating at the second diffraction by only adjusting the distance between the RP and the grating. The OC can be mounted in the central area of the whole SBC configuration and the distance between the rear facet of laser emitters and the OC is shortened. The main advantages are as follows: 1) the SBC source is miniaturized, 2) the SBC structure is more stable, 3) the SBC linewidth is narrowed by nearly one-half, and 4) the grating adjustment is simplified. In this work, similar combined power and beam quality but half of the spectral width and a smaller volume are obtained by comparing the standard SBC with the proposed SBC of the same 800 nm laser bar.

2. Experimental setup

A standard SBC setup with a TG is shown in Fig. 1(a). The external resonator is composed of the rear facet of the laser diode array (LDA) and the OC. The anti-reflection (AR) coating front facet of the LDA and the TG are respectively located on the front and rear focal planes of the TL with the focal length f_T . All the beams from the LDA spatially overlap on the TG at different incident angles, diffract at the same angle, and are perpendicular to the OC. The TG is placed in the Littrow configuration with respect to the central ray of the LDA propagating along the original optical axis oz of the external resonator to obtain the highest diffraction efficiency. The SBC linewidth $\Delta\lambda_{SBC}$ is given by $\Delta\lambda_{SBC} \approx d \cdot \Lambda \cdot \cos\theta_L / f_T$ [4], in which, d is the LDA size in the SBC direction, Λ is the grating period and θ_L is the Littrow angle.

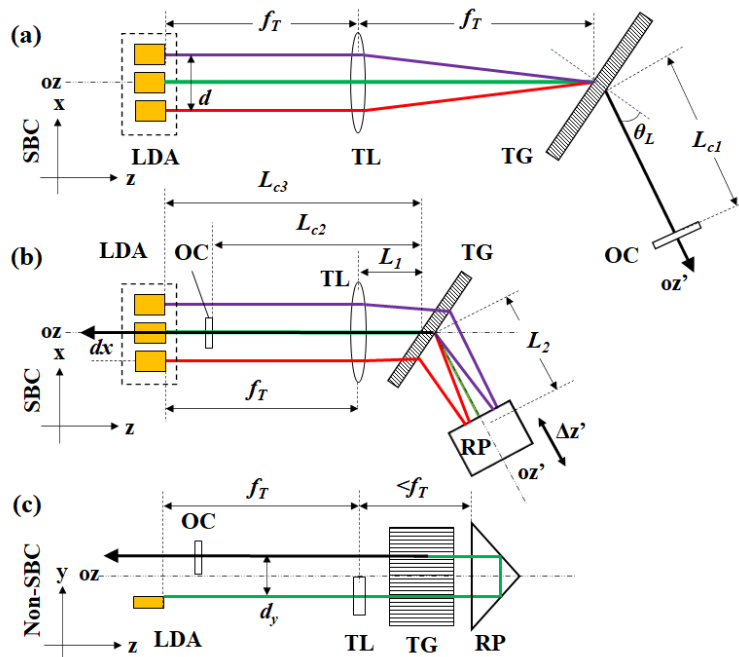


Fig. 1. Setup for (a) standard SBC configuration with a TG in the SBC direction, (b) ESBC configuration in the SBC direction, and (c) ESBC configuration in the non-SBC direction.

An extended SBC (ESBC) configuration is built by introducing an RP, as shown in Fig. 1(b) - (c). In the SBC direction, the external resonator is also composed of the rear cavity surface of the LDA and the OC, and the TG is placed in Littrow configuration with respect to oz . The front facet of the LDA is still located on the front focal plane of the TL. But the TG is closer to the TL, and the interval L_1 between the TL and the TG is smaller than f_T . The diffracted beams vertically hit on the inclined plane of the RP along the diffraction optical axis oz' . After two reflections by the right angle planes of the RP, the central beam propagates backward to the TG at the incident angle of θ_L , and the second diffraction occurs. At the same time, all the beams spatially overlap on the TG by moving the RP along oz' , diffract at the same angle of θ_L , and perpendicularly strike onto the OC eventually along oz . The OC is located in the middle area of the SBC source and the emitting direction of the combining laser coincides with the original optical axis oz . In the non-SBC direction, a displacement of d_y between the LDA beam and the SBC laser is generated by using the RP, which enables the combining laser to fold into the SBC cavity. This way effectively reduces the size of the SBC direction. Therefore, the ESBC structural stability could be improved owing to the more compact structure, the shorter distance between the two cavity mirrors and the more stable OC, comparing with the standard SBC configuration [11]. The double diffractions of the TG also enhance the dispersion ability twice. This improvement compresses the linewidth to one-half that of the standard SBC setup, and the corresponding linewidth $\Delta\lambda_{ESBC}$ is $\Delta\lambda_{ESBC} = \Delta\lambda_{SBC}/2 \approx d^* \Lambda \cos\theta_L / f_T / 2$. Due to the influence of the grating diffraction, an approximate relationship exists between f_T and the optical path of $(L_1 + d_y + 2^* L_2)$, $f_T = (L_1 + (d_y + 2^* L_2)) / 2$, where L_2 represents the distance between the TG and the reflection position on the RP.

An 800 nm diode laser bar with AR coating of $R_f < 0.5\%$ at the front facet is used, including 19 emitters. Each emitter is 100 μm wide and 1 μm thick with 500 μm period. A beam transformation system (BTS) from Limo, with the fast axis collimator (FAC) focal length of $f_F = 365 \mu\text{m}$ and the period of 500 μm , is employed to collimate the fast axis beam and rotate every emitter beam by 90° . Due to the beam transform effect of the BTS, the laser bar is spectrally combined in the fast axis direction. A cylindrical lens with a focal length of $f_s = 54 \text{ mm}$ is applied to collimate the slow axis beam. In Fig. 1(a), a transform cylindrical lens with a focal length of $f_T = 300 \text{ mm}$ is placed 300 mm away from the image of the laser bar after the BTS and the TG. This way spatially overlaps all of the laser emitters onto the TG. A -1^{st} order TG, with the period of $\Lambda = 543 \text{ nm}$ ($\Lambda^{-1} = 1841.6 \text{ lines/mm}$), is placed in Littrow configuration with respect to the central emitter ray of the 800 nm bar. Specifically, the TG is made from fused silica with an optimized diffraction efficiency of over 99% for S-polarized light within the spectral range from 790 nm to 810 nm. A $\lambda/2$ plate is inserted to rotate the TE-polarized laser beam of the laser bar into S polarization with respect to the plane of incidence at the TG. The reflectivity of the OC is chosen to be \sim nearly 9%. The OC is positioned with a distance of $L_{C1} = 250 \text{ mm}$ behind the TG to reduce crosstalk effects.

In Fig. 1(b), the TG is mounted behind the TL with the interval of $L_1 = 200 \text{ mm}$. An additional RP is employed to translate the laser beam in the non-SBC direction with the displacement of $d_y = 10 \text{ mm}$, as shown in Fig. 1(c). The RP has the AR coating of $R_i < 0.1\%$ on the inclined plane and the right angle plane size of 30 mm \times 30 mm. The interval L_2 is about 95 mm. The laser beams from the LDA pass through the TG twice and overlap on the TG at the second time. Both the incident angle and the diffraction angle are equal to θ_L of the TG. The reflectivity of the OC is chosen to be \sim approximately 9%. The distance L_{C3} between the TG and the LDA facet is about 500 mm in the SBC direction according to the location relationship. Consequently, the OC can be placed behind the TG within a wide adjustment range of 0 - 500 mm without occupying the additional space. The distance L_{C2} between the TG and the OC is eventually set to 400 mm, which is longer than that of the standard SBC structure because of the smaller spectral spacing. However, the overall size is still smaller in the SBC direction even if L_{C2} is further extended to 500 mm. The laser power is measured using a pyroelectric power meter (Ophir FL500A). The

output spectrum is recorded with a fiber optic spectrum analyzer (Yokogawa AQ6370D) sampled by an integrating sphere. The beam quality is surveyed with an M^2 measurement system based on a camera beam profiler (Thorlabs M2MS).

3. Experimental results and analysis

The continuous-wave (CW) power P and electro-optical (E-O) conversion efficiency η_{EO} of free running (FR), SBC and ESBC as a function of the current at the coolant temperature of 20 °C are shown in Fig. 2. With the help of the external feedback, both of the threshold currents of SBC and ESBC are reduced to 8 A, while that of FR is 14 A. At the current of 40 A, the CW power and E-O conversion efficiency are $P_{FR} = 27.47$ W and $\eta_{EO-FR} = 40.5\%$ for FR, $P_{SBC} = 28.53$ W and $\eta_{EO-SBC} = 42.1\%$ for SBC, and $P_{ESBC} = 27.15$ W and $\eta_{EO-ESBC} = 40.1\%$ for ESBC, respectively. The respective maximum E-O conversion efficiency values are 43.1% and 41.6% for SBC and ESBC at 35 A. The combining efficiency η_c , defined as the ratio of the combining power to P_{FR} , is $\eta_{c-SBC} = 103.86\%$ and $\eta_{c-ESBC} = 98.84\%$ at 40 A for SBC and ESBC, respectively.

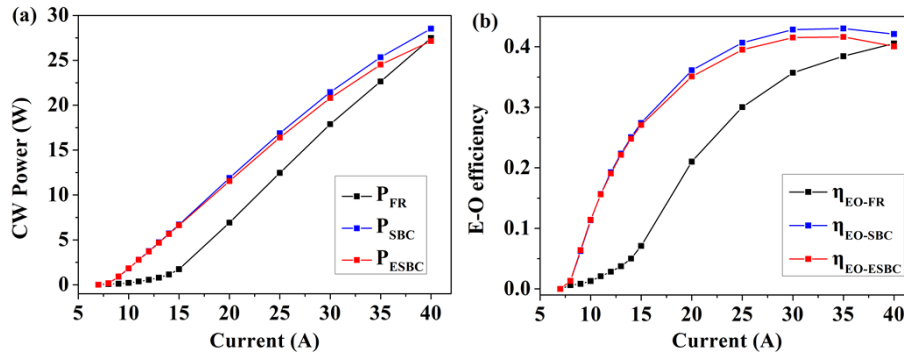


Fig. 2. (a) CW power and (b) E-O conversion efficiency of FR, SBC and ESBC

The CW power ratio of P_{ESBC} and P_{SBC} as a function of current is shown in Fig. 3. At the current from 8 A to 15 A, both of the combining power are similar and the ratio of P_{ESBC}/P_{SBC} is close to 1. However, the power ratio drops gradually as the current increases and decreases to 95% at 40 A. The power drop could be explained by the reduced effective feedback because of the insufficient aperture of the grating, and a TG with a larger size would help to slow down the power drop.

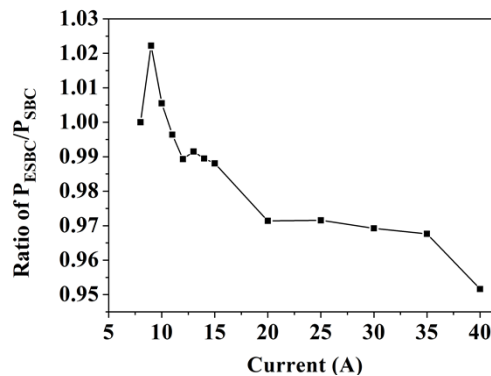


Fig. 3. Curve of CW power ratio of P_{ESBC}/P_{SBC}

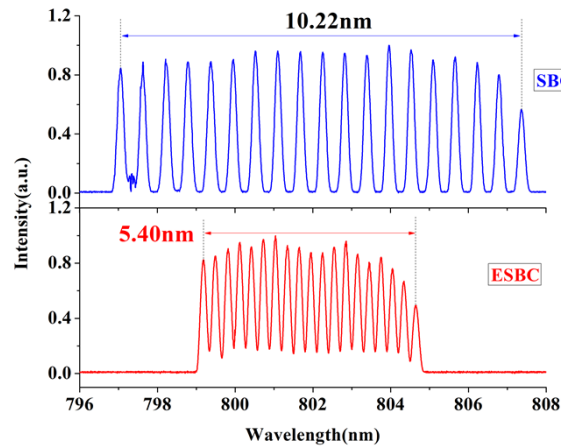


Fig. 4. Combining spectrum of SBC and ESBC at the current of 35 A.

Figure 4 demonstrates the combined spectral distribution of SBC and ESBC at the current of 35 A. For both of these cases, 19 spectral peaks can be obviously distinguished. The interval between minimum and maximum wavelength peaks are 10.22 nm and 5.40 nm for SBC and ESBC, respectively. These values agree with the corresponding theoretical design values of 10.99 nm and 5.50 nm. A possible reason for the small discrepancies of 7.0% and 1.8% is a higher angular dispersion of the grating if the angle of incidence of the central emitter upon the grating differs from θ_L . A small cross-talk is observed in the SBC spectrum, which means a longer distance of L_{C1} is required.

At the current of 35 A, beam qualities of SBC and ESBC are measured in Fig. 5 by the justification criterion of clip level at $1/e^2$. The x-axis is the fast axis, which is also the SBC

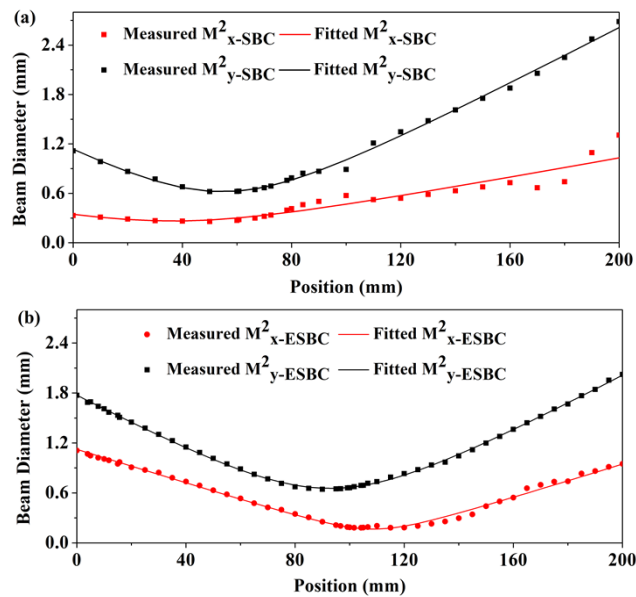


Fig. 5. Beam quality of (a) SBC and (b) ESBC at the current of 35 A

direction, and the y-axis is the slow axis. For SBC, M^2_{x-SBC} and M^2_{y-SBC} are 1.51 and 10.59, respectively. For ESBC, M^2_{x-ESBC} and M^2_{y-ESBC} are 1.61 and 11.41, respectively. Compared with the beam qualities of SBC and ESBC, the beam quality deteriorations of 6.21% and 7.19% are calculated, defined by $(M^2_{ESBC} - M^2_{SBC}) / M^2_{ESBC}$, which may be caused by the alignment error and the dispersion effect. These conditions result in the incomplete coincidence on the grating.

4. Conclusion

An ESBC structure that folds the optical path of the combining laser into the non-SBC direction and doubly compresses the SBC spectrum by introducing an RP is demonstrated. An obvious advantage is that the OC can be physically installed in the central area of the SBC source, which improves the SBC structural stability. The size of the SBC dimension can also be effectively reduced, which provides a way for miniaturization of the SBC laser source. A narrower SBC spectral width can be achieved as well by multiplexing the single grating, which obtains a higher SBC power by combining more laser emitters within the same spectral range. Eventually, similar combined power and beam quality but half of the spectral width and a smaller size are demonstrated by employing the proposed SBC structure with the same 800 nm laser bar, which are consistent with the theoretical analysis results.

Funding. National Natural Science Foundation of China (61991433, 62121005); Chinese Academy of Sciences Key Project (XDB43030302); Equipment pre research (2006ZYG0304); Foundation strengthening project (2020-JCJQ-ZD-245-11).

Disclosures. The authors declare no conflicts of interest.

Data availability. No data were generated or analyzed in the presented research.

References

1. M. Haas, S. Rauch, S. Nagel, L. Irmler, T. Dekorsy, and H. Zimer, "Thin-film filter wavelength-stabilized, grating combined, high-brightness kW-class direct diode laser," *Opt. Express* **25**(15), 17657–17670 (2017).
2. B. Chann, F. Villarreal, W. Zhou, J. Roethle, A. Guiterrez, M. Sauter, C. Halle, S. Domoto, and B. Lochman, "Advances in blue high-power/high-brightness direct diode lasers using wavelength beam combining," *Proc. SPIE* **PC11983**, PC1198307 (2022).
3. C. C. Cook and T. Y. Fan, "Spectral Beam Combining of Yb-doped Fiber Lasers in an External Cavity," in *Advanced Solid State Lasers*, M. Fejer, H. Injeyan, and U. Keller, eds., Vol. 26 of OSA Trends in Optics and Photonics (Optical Society of America, 1999), paper PD5.
4. V. Daneu, A. Sanchez, T. Y. Fan, H. K. Choi, G. W. Turner, and C. C. Cook, "Spectral beam combining of a broad-stripe diode laser array in an external cavity," *Opt. Lett.* **25**(6), 405–407 (2000).
5. R. K. Huang, B. Chann, J. Burgess, B. Lochman, W. Zhou, M. Cruz, R. Cook, D. Dugmore, J. Shattuck, and P. Tayebati, "TeraDiode's high brightness semiconductor lasers," *Proc. SPIE* **9730**, 97300C (2015).
6. F. Villarreal, W. Zhou, J. Roethle, M. Sauter, K. Inoue, B. Lochman, and B. Chann, "Advances in blue and near-IR high-power/high-brightness direct diode lasers using wavelength beam combining," *Proc. SPIE* **11262**, 112620U (2020).
7. H. Yu, S. Tan, H. Pan, S. Sun, and J. Li, "Development of a 350 W, 50 μm , 0.15 numerical aperture (NA) wavelength stabilized fiber coupled laser diode module for pumping Yb-doped fiber laser," *Proc. SPIE* **11262**, 112620 V (2020).
8. Z. Zhu, M. Jiang, S. Cheng, Y. Hui, H. Lei, and Q. Li, "Narrow linewidth operation of a spectral beam combined diode laser bar," *Appl. Opt.* **55**(12), 3294–3296 (2016).
9. B. Wang, W. Guo, Z. Guo, D. Xu, J. Zhu, Q. Zhang, T. Yang, and X. Chen, "Spectral beam combining of multi-single emitters," *Proc. SPIE* **9733**, 97330F (2016).
10. M. Haas, S. Rauch, S. Nagel, R. Beißwanger, T. Dekorsy, and H. Zimer, "Beam Quality Deterioration in Dense Wavelength Beam-Combined Broad-Area Diode Lasers," *IEEE J. Quantum Electron.* **53**(3), 1–11 (2017).
11. V. Magni, "Resonators for solid-state lasers with large-volume fundamental mode and high alignment stability," *Applied Optics* **25**(1), 107–117 (1986).